Supporting Information

Photo-Enhanced Piezocatalytic Hydrogen Evolution by In Situ Silver Piezodeposited Scheelite–type $BaMoO_4$ and $BaWO_4$

Talha Kuru[a], Adem Sarilmaz[b], Emre Aslan[c], Faruk Ozel[*b], Imren Hatay Patir[*a]

Band-gap Calculation

The band-gap values and types of piezo-catalysts were determined by following the steps below.[1-4]

1. Diffuse reflection measurements were performed to investigate optical properties and band-gap calculations.
2. Absorption ($F(R_\infty)$) was calculated using the Kubelka-Munk equation ($F(R_\infty)=(1-R_\infty)^2/2R_\infty$).
3. Approximately band-gaps were estimated by plotting $d[\ln(F(R_\infty)h\upsilon)]/[h\upsilon]$ vs. photon energy graphs ($BaMoO_4$: 3.01 eV and $BaWO_4$: 2.96 eV).
4. Approximately band gaps were used to determine the m exponent in the Tauc equation ($F(R_\infty)h\upsilon = A(h\upsilon-Eg)^m$). $\ln(F(R_\infty)h\upsilon)$ vs. $\ln(h\upsilon-Eg)$ graphs were plotted, and m exponents were determined from the slope of the plot ($BaMoO_4$: 0.399 and $BaWO_4$: 0.409). These values are close to 0.5 indicating that piezo-catalysts have the direct band transition type.
5. The band-gaps were calculated by plotting $(F(R_\infty)h\upsilon)^2$ vs. photon energy graphs ($BaMoO_4$: 3.32 eV and $BaWO_4$: 2.93 eV).

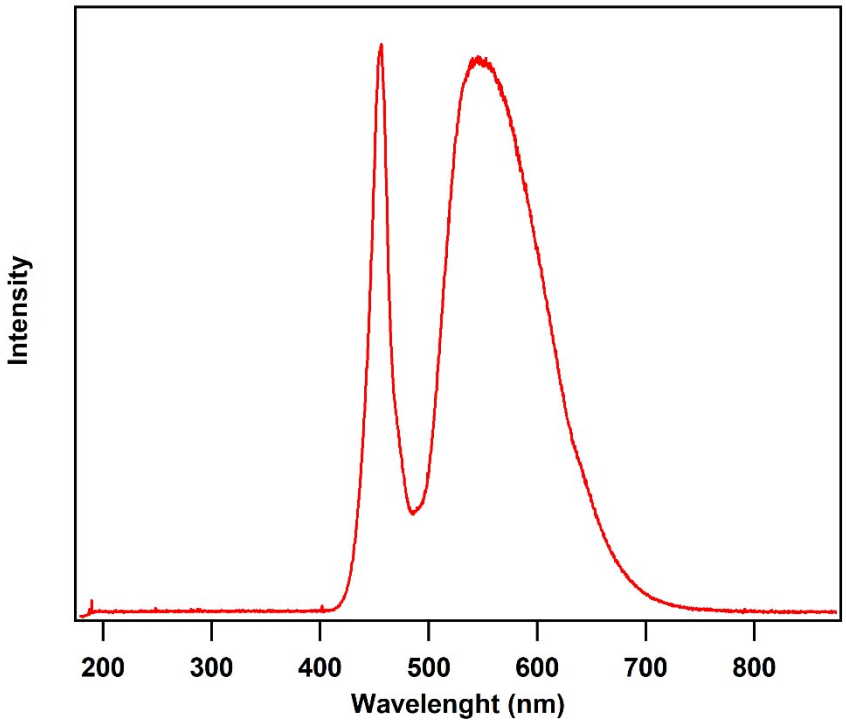

Figure S1. White LED light spectrum

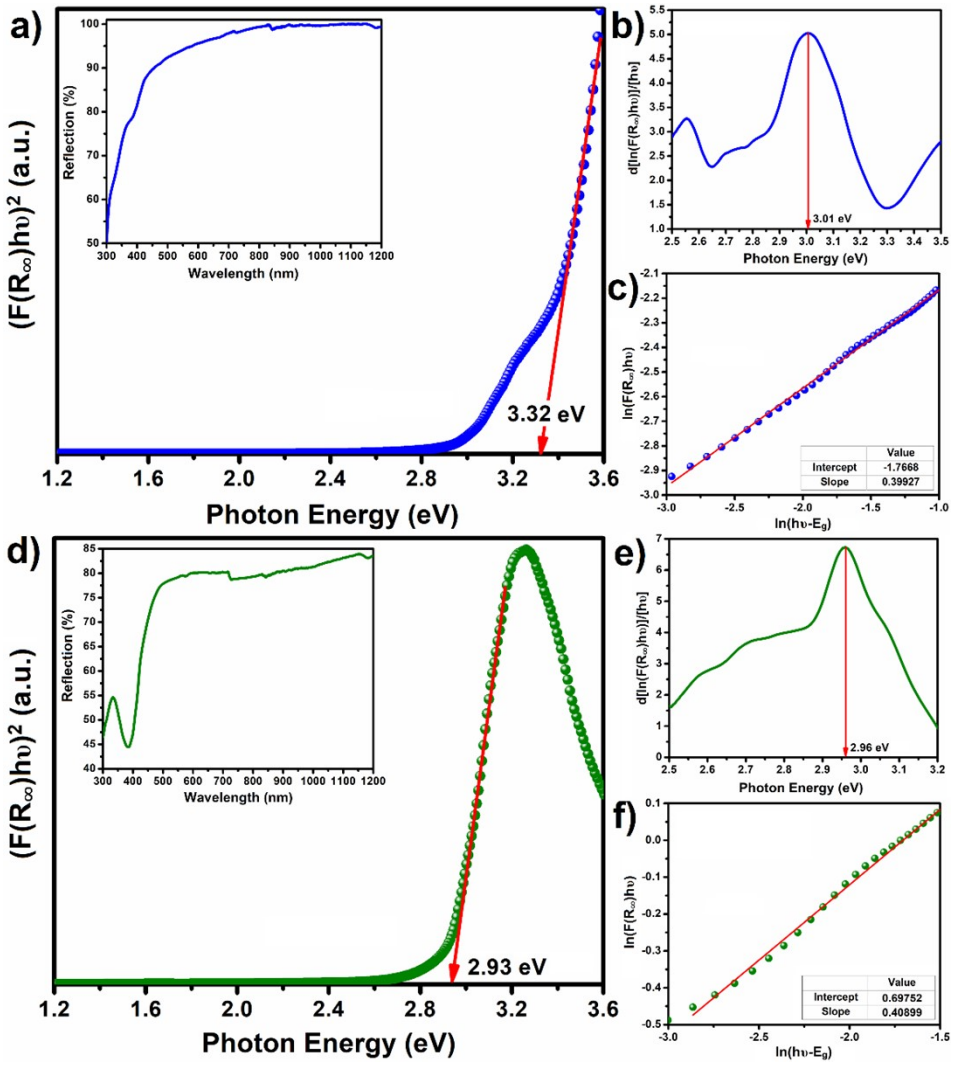

Figure S2. Band-gap energy graphs **(a,d)**, d[ln(F(R∞)hu)]/[hu] vs. photon energy graphs **(b,e)**, ln(F(R∞)hu) vs. ln(hu-Eg) graphs **(c,f)** of $BaMoO_4$ **(a-c)** and $BaWO_4$ **(d-f)**. Diffuse reflection graphs were given as an inset figure in the band-gap energy diagrams.

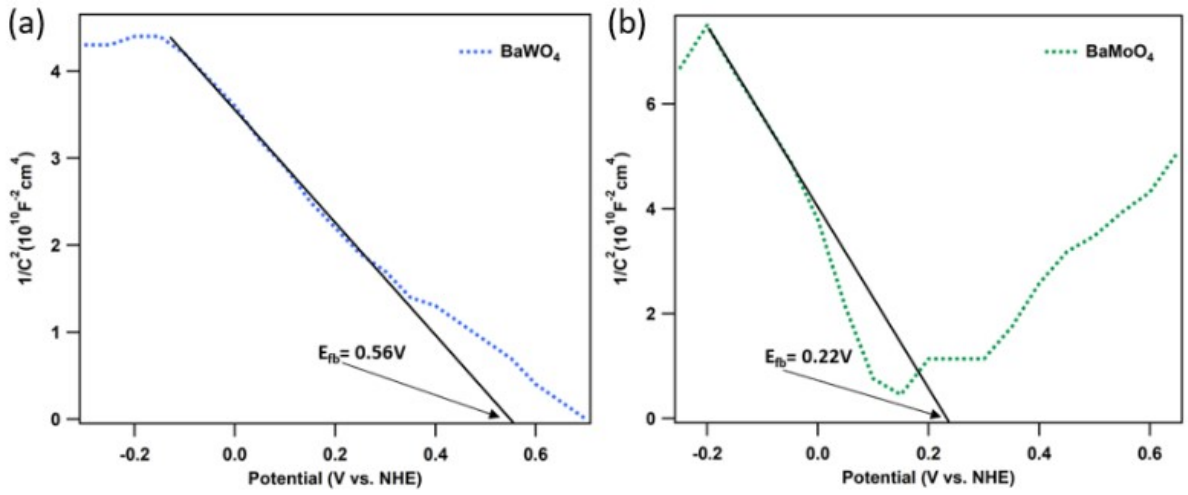

Figure S3. Mott-Schottky plots of **(a)** $BaWO_4$ and **(b)** $BaMoO_4$ in 0.1M $NaSO_4$. V vs. NHE at pH=7

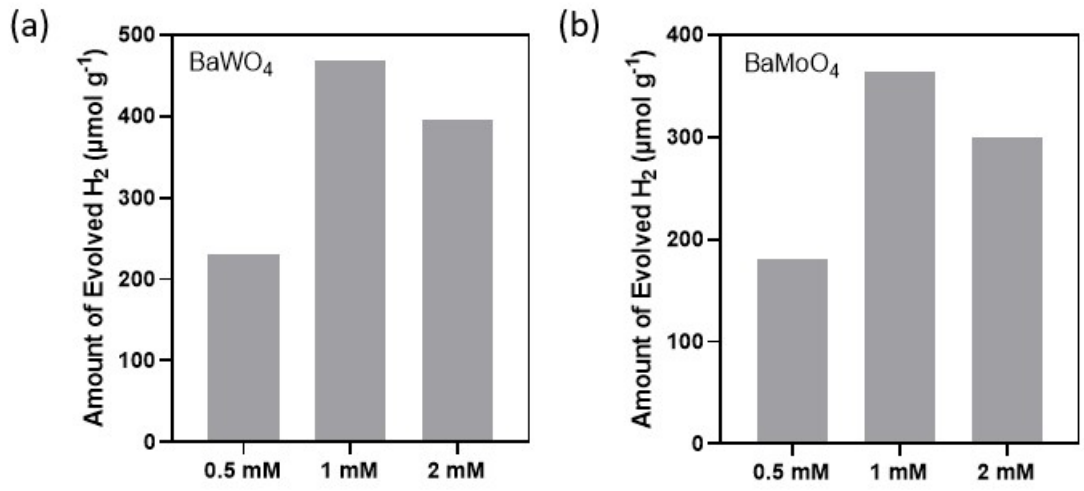

Figure S4. Piezocatalytic hydrogen production results of **(a)** $BaWO_4$ and **(b)** $BaMoO_4$ depending on Ag piezodeposition at 0.5, 1 and 2 mM $AgNO_3$ concentrations

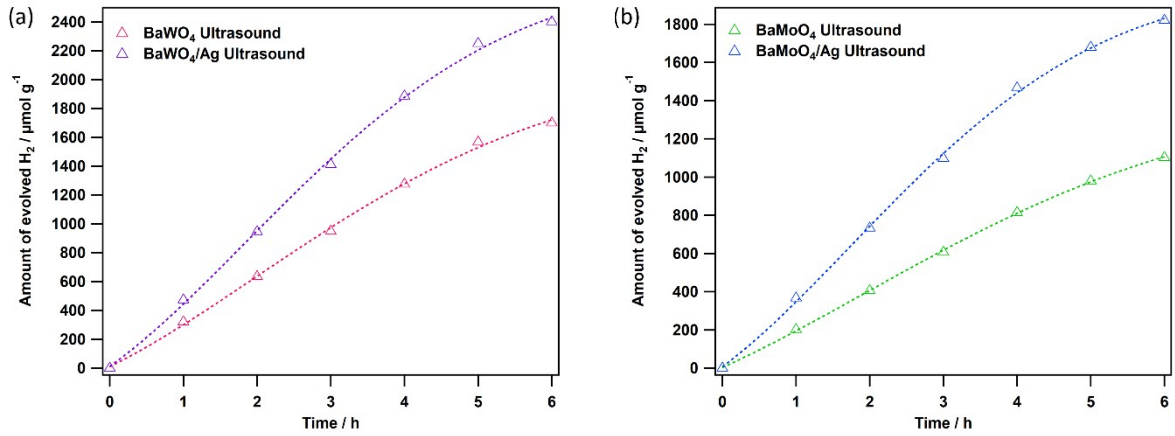

Figure S5. The piezocatalytic hydrogen production of **(a)** $BaWO_4$, $BaWO_4$/Ag, **(b)** $BaMoO_4$ and $BaMoO_4$/Ag for 6 hour.

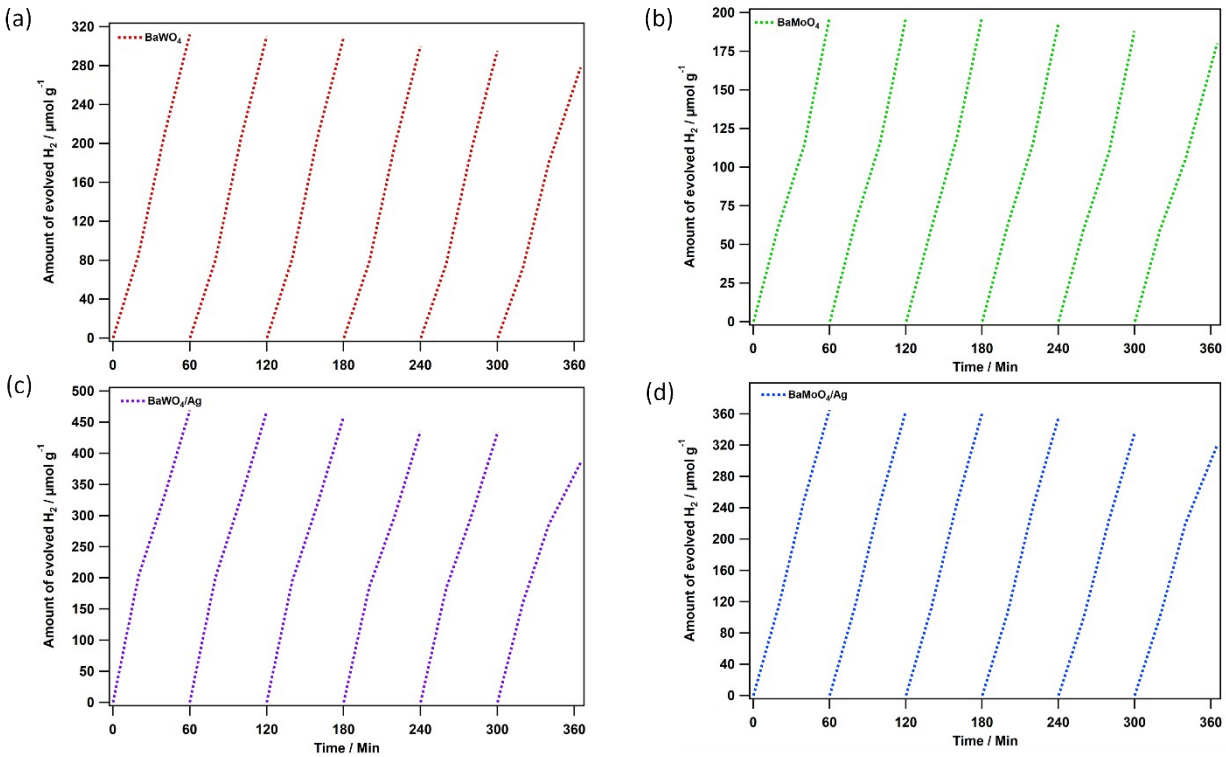

Figure S6. Reusability experiments for piezocatalytic hydrogen production of **(a)** $BaWO_4$, **(b)** $BaMoO_4$, **(c)** $BaWO_4$/Ag and **(d)** $BaMoO_4$/Ag for 6 cycles

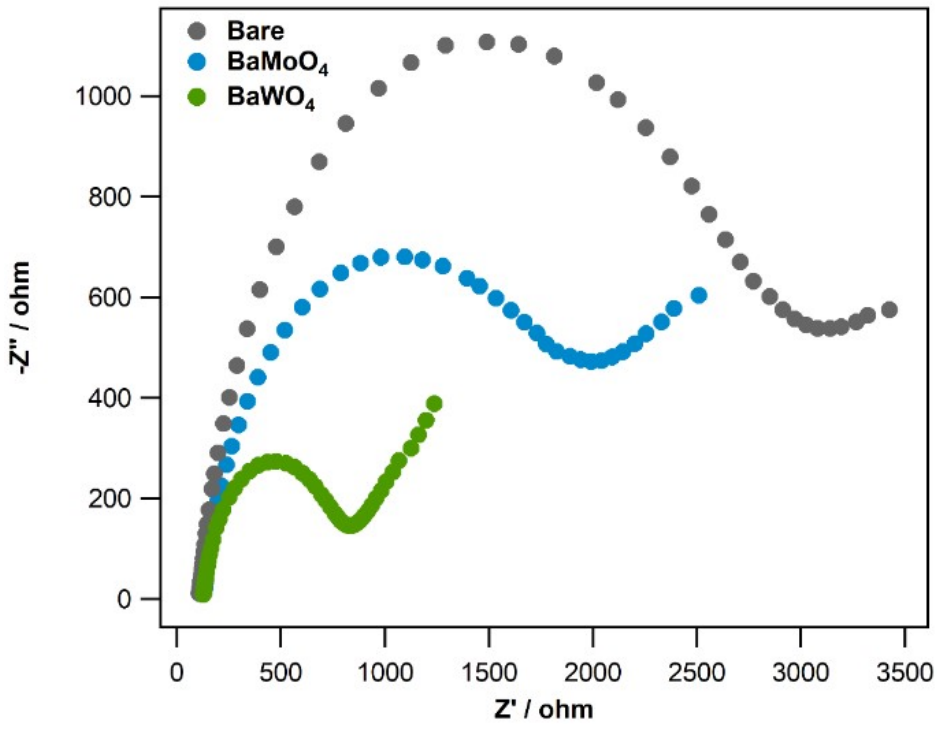

Figure S7. Nyquist plots of $BaMoO_4$ and $BaWO_4$ from Electrochemical Impedance Spectroscopy (EIS).

Table S1. Comparison of H_2 production rates of different piezocatalysts

Catalyst	Catalytic Condition	Scavenger	H_2 production	Ref
ZnS nanosheet	Ultrasonic: 100 W 27 kHz	Pure Water	1080 μmol h^{-1} g^{-1}	5
$BaTiO_3$ nanoparticle	Ultrasonic: 100 W 40 kHz	15% TEOA	2 μmol h^{-1} g^{-1}	6
$BaTiO_3$ nanowire	Ultrasonic: 100 W 40 kHz	15% TEOA	18 μmol h^{-1} g^{-1}	6
$BaTiO_3$ nanosheet	Ultrasonic: 100 W 40 kHz	15% TEOA	92 μmol h^{-1} g^{-1}	6
Bi_2WO_6 nanoplate	Ultrasonic: 40 kHz	20% TEOA	191 μmol h^{-1} mg^{-1}	7
CdS nanosheet	Ultrasonic: 50 kHz	Na_2S/Na_2SO_3	144 μmol h^{-1} mg^{-1}	8
CdS nanosheet	Ultrasonic: 50 kHz Light: 300 W Xe lamp	Na_2S/Na_2SO_3	633 μmol h^{-1} mg^{-1}	8
bulk g-C_3N_4	Ultrasonic: 250 W 40 kHz	0.1 M Glucose	2690 μmol g^{-1} h^{-1}	9
Ultra thin g-C_3N_4	Ultrasonic: 250 W 40 kHz	0.1 M Glucose	8350 μmol g^{-1} h^{-1}	9
Ultra thin g-C_3N_4	Ultrasonic: 50 kHz Light: λ ≥ 420 nm	0.1 M Glucose	12160 μmol g^{-1} h^{-1}	9
$BaWO_4$	Ultrasonic: 50 kHz	5% TEOA, pH = 9	312.58 μmol g^{-1} h^{-1}	**This Work**
$BaMoO_4$	Ultrasonic: 50 kHz	5% TEOA, pH = 9	197.97 μmol g^{-1} h^{-1}	**This Work**
$BaWO_4$	Ultrasonic: 50 kHz Light: White LED Light, λ ≥ 420 nm	5% TEOA, pH = 9	1103 μmol g^{-1} h^{-1}	**This Work**
$BaMoO_4$	Ultrasonic: 50 kHz Light: White LED Light, λ ≥ 420 nm	5% TEOA, pH = 9	788.76 μmol g^{-1} h^{-1}	**This Work**

References

1. A. Sarilmaz, G. Yanalak, E. Aslan, F. Ozel, I. H. Patir and M. Ersoz, *Renewable Energy*, 2021, **164**, 254-259.
2. G. Yanalak, A. Sarılmaz, G. Karanfil, E. Aslan, F. Ozel and I. H. Patir, *Journal of Photochemistry and Photobiology A: Chemistry*, 2020, **394**, 112462.
3. T. L. Le, S. Guillemet-Fritsch, P. Dufour and C. Tenailleau, *Thin Solid Films*, 2016, **612**, 14-21.
4. M. Borah and D. Mohanta, *Journal of Applied Physics*, 2012, **112**.
5. W. Feng, J. Yuan, L. Zhang, W. Hu, Z. Wu, X. Wang, X. Huang, P. Liu and S. Zhang, *Applied Catalysis B: Environmental*, 2020, **277**, 119250.
6. C. Yu, M. Tan, Y. Li, C. Liu, R. Yin, H. Meng, Y. Su, L. Qiao and Y. Bai, *Journal of Colloid and Interface Science*, 2021, **596**, 288-296.
7. X. Xu, L. Xiao, Z. Wu, Y. Jia, X. Ye, F. Wang, B. Yuan, Y. Yu, H. Huang and G. Zou, *Nano Energy*, 2020, **78**, 105351.
8. Y. Zhao, X. Huang, F. Gao, L. Zhang, Q. Tian, Z.-B. Fang and P. Liu, *Nanoscale*, 2019, **11**, 9085-9090.
9. C. Hu, F. Chen, Y. Wang, N. Tian, T. Ma, Y. Zhang and H. Huang, *Advanced Materials*, 2021, **33**, 2101751.